

## Guided-wave modes in graded-index optical fibers by two-point quasi-rational approximants

E. Castro\*, P. Martín, J. Puerta, and C. Cereceda  
*Departamento de Física, Universidad Simón Bolívar,*  
*Apartado 89000, Caracas 1080A, Venezuela,*  
*\*e-mail: ecastro@usb.ve*

Recibido el 8 de marzo de 2005; aceptado el 7 de febrero de 2006

Approximated analytic solutions for wave propagation in graded-index optical fiber have been found in the case of a parabolic profile. Approximants with high accuracy are presented that are much better than those found by other authors. A two-point quasi-rational method and two-point Padé approximants are used in this work. The approximants are explicitly determined for the azimuthal eigenvalues  $l = 0, 1, 2$  and the  $m$ th mode numbers  $m = 0, 1, 2, 3$ .

*Keywords:* Two-point quasi-rational approximants; graded-index fibres; waveguide propagation and eigenmode analysis.

En el presente trabajo, se obtuvieron soluciones analíticas aproximadas para la propagación de ondas en fibras ópticas con índice gradual en el caso de perfil parabólico. Los aproximantes obtenidos resultaron ser más precisos que aquellas aproximaciones halladas previamente por otros autores. En este trabajo se usaron los aproximantes cuasi-rationales a dos puntos y los aproximantes de Padé. Se determinaron explícitamente los determinantes para los autovalores azimutales  $l = 0, 1, 2$  y los modos  $m = 0, 1, 2, 3$ .

*Descriptores:* Aproximantes cuasi-rationales a dos puntos; fibras ópticas de índice graduado; propagación en guías de ondas y análisis de los modos normales.

PACS: 02.30.Mv, 42.81.Qb, 42.81.Ht

### 1. Introduction

An optical fiber waveguide is made of a glass core surrounded by a lower-index cladding. These are low-loss optical waveguides and are valuable in optical communications and other closely related fields [1-7].

Graded-index waveguides display relatively little transit-time variation and it is possible to transmit very large electrical bandwidths. These waveguides are made with a refractive index that decreases gradually with the distance from the axis of the optical fiber. The rays in an optical fiber such as this one travel in curved paths. If a graded-index optical fiber is made with a correct index profile, this can greatly suppress modal dispersion, and consequently reduce group delay. The modes in a graded-index optical fiber are more confined to the core of the guide than those in a step-index optical fiber.

For most experimental applications, it is useful to make the assumption that the true profile will not deviate much from the perfect parabolic profile [1]. In a step-index optical fiber, the modal spacing increases linearly with an increasing mode order. For a parabolic index profile, modal spacing is independent of the mode number.

As is well known, Whittaker functions [4] are the solution for the unbounded case; however, here we are interested in an optical fiber of finite radius, that is, the bounded case where  $r \leq a$ .

Exact solutions cannot be obtained for the case we are interested in. Instead, the problem is treated using simple ray analysis; numerical calculations for each particular case are usually required [8]. Approximated solutions are presented here that can be used instead of the numerical solutions, be-

cause of the high accuracy of the results, sufficient for most applications. These solutions are different from those found with the WKB-method, which is usually used for graded-index optical fibers [1,9].

The two-point quasi-rational approximation method used here is an improvement on the two-point Padé method [10], and was applied initially in the computation of the plasma dispersion function [11], and later for other different areas such as Coulomb scattering [12], quantum field theory [13], special functions [14-21], classical mechanics [22], solid state physics [23], quantum mechanics [24], applied optics (transmittance calculations by circular apertures) [25,26]. This list of references, though incomplete, gives a good idea of the method used here and its applications.

In this paper, the solution is formed by using, simultaneously, the boundary conditions at the center of the optical fiber and a simplified boundary condition at its surface. The solutions found here are good either close to or far from the cutoff. However, in order to find the approximated solutions, a simplification of the boundary conditions at the core surface has been used. The solution on the core must be coupled with the solution at the cladding, which in most cases can be represented by the modified Bessel functions, assuming that the energy irradiated outside the cladding is neglected. The simplification performed here is for cases in which the energy in the cladding is much smaller than that in the core. In this case, the energy in the cladding could also be neglected and the scalar treatment of the wave amplitude, the field functions will be approximately zero at the surface. This condition has been imposed on the asymptotic series to be used in order to obtain the two-point quasi-rational approximants found here.

Approximated solutions for wave propagation have been found for multimode optical fibers with parabolic profiles for different values of  $l = 0, 1, 2$  and  $m = 0, 1, 2, 3$ , where  $l$  is the azimuthal eigenvalue and  $m$  is associated with the  $m$ th mode number. However, the procedure followed here can be used for different values of  $l$  and  $m$  than those specified here. The form of our approximants is the same for all modes.

In this work, two methods have been applied in order to obtain the approximants: two-point quasi-rational method, and two-point Padé method. However, in the main text only the former is described in detail because the results are much better than the latter. The two-point Padé results are considered in detail in the Appendix, and they are compared to the main one. It is convenient to remember that the two-point quasi-rational method is applied there in order to determine suitable auxiliary functions as well as a suitable independent variable (here exponential) in order to connect the power series and the asymptotic expansion.

As is detailed bellow, our results are good for all values of  $r$  and characteristic parameters. There is no need to require slow index variation, as happens when the WKB method of approximation is used. Furthermore, the zeroth WKB approximation is good only for the ray optic treatment, where the phase changes at the caustic or turning points are ignored and, at the caustic point, the first-order WKB results fail. At the turning point, the slope of the ray path changes sign, and the ray bends toward the axis as a result of total internal reflection.

An important feature of the approximants is that they can be derived or integrated symbolically, and the results will be correct due to the high accuracy obtained. It is interesting to point out that although the parabolic profile has been considered, the method described here can also be applied to other patterns of graded index optical fibers.

The paper is organized as follows. In Sec. 2, we determine the values of the parameters for the power series and the asymptotic expansions. In Sec. 3, we discuss the procedure to obtain the two-point quasi-rational approximants. In Sec. 4, an analysis and discussion of results of the various approximants are presented. Section 5 is devoted to conclusions.

## 2. Suitable expansions of the scalar field solutions for graded- index optical fibers

The scalar field equation in cylindrical coordinates[1] is:

$$\frac{d^2 \tilde{\Psi}}{dr^2} + \frac{1}{r} \frac{d\tilde{\Psi}}{dr} + \frac{1}{r^2} \frac{d^2 \tilde{\Psi}}{d\theta^2} + \frac{d^2 \tilde{\Psi}}{dz^2} + k_0^2 n^2(r) \tilde{\Psi} = 0;$$

$$k_0 = \frac{2\pi}{\lambda_0}, \quad (1)$$

where  $k_0$  and  $\lambda_0$  are the wave number and wave length in the vacuum respectively, and  $n^2(r)$  is the optic-index profile of the optical fiber.

Because of the axial and circular symmetry of the wave, the wave solution has the form

$$\tilde{\Psi}(r, \theta, z) = \tilde{\Psi}(r) \exp [i(l\theta + \beta z)], \quad (2)$$

where  $\beta$  is the propagation wave number along  $z$  and  $l$  is an integer number, called the azimuthal eigenvalue. Thus, Eq. [1] becomes

$$\frac{d^2 \Psi(r)}{dr^2} + \frac{1}{r} \frac{d\Psi(r)}{dr} + \left[ k_0^2 n^2(r) - \beta^2 - \frac{l^2}{r^2} \right] \Psi(r) = 0. \quad (3)$$

For this paper, a parabolic profile will be assumed, that is,

$$n^2(r) = n_0^2 \left[ 1 - 2 \Delta \left( \frac{r}{a} \right)^2 \right], \quad (4)$$

where  $\Delta$  is the relative refractive index difference between core and cladding, and depends on the core index  $n_0$  and cladding index  $n_c$  as

$$\Delta = \frac{n_0^2 - n_c^2}{2n_0^2}. \quad (5)$$

The dimensionless independent variable  $\rho$  will be used

$$\rho = \frac{r}{a}. \quad (6)$$

Thus the differential equation can be written as

$$\frac{d^2 \phi(\rho)}{d\rho^2} + \frac{1}{\rho} \frac{d\phi(\rho)}{d\rho} + \left[ g_1 - g_2 \rho^2 - \frac{l^2}{\rho^2} \right] \phi(\rho) = 0, \quad (7)$$

where the parameters  $g_1$  and  $g_2$  denote

$$g_1 = a^2 (k_0^2 n_0^2 - \beta^2), \quad g_2 = 2\Delta a^2 k_0^2 n_0^2. \quad (8)$$

In this paper, two ways have been used to find approximate solutions for this function  $\phi(\rho)$ :

- 1) the two-point quasi-rational method, and
- 2) the two-point Padé method.

However the results of the first method are much better than those of the second method, which will only be shown briefly in Appendix A.

For the two-point quasi-rational method, the range of interest  $(0, 1)$  for  $\rho$  must be extended to the range  $(0, \infty)$ , in order to have a power series around zero and an asymptotic expansion around infinity. There are several possibilities for this transformation; however, we have found good results using the following change of variable:

$$\rho = 1 - e^{-y}, \quad (9)$$

which gives the new differential equation

$$\frac{d^2 \Psi(y)}{dy^2} + \frac{1}{(1 - e^{-y})} \frac{d\Psi(y)}{dy} + e^{-2y} \times \left[ g_1 - g_2 (1 - e^{-y})^2 - \frac{l^2}{(1 - e^{-y})^2} \right] \Psi(y) = 0, \quad (10)$$

where  $\phi(\rho) = \Psi(y)$ . This change of variables is done in such a way that for  $\rho = 0, y = 0$  and, for  $\rho = 1, y = \infty$ . The power series are easily obtained by the Frobenius method as

$$\Psi_p(y) = y^l \sum_{i=0}^{\infty} a_i y^i, \tag{11}$$

where the  $a_i$ 's are given in Table I for each mode with values of  $l$  from 0 to 2 and  $m = 0, 1, 2, 3$ , and for experimental parameters: core index  $n_0 = 1.5$ , cladding index  $n_c = 1.485$ , core radius  $a = 5\mu\text{m}$ , length wave  $\lambda_0 = 1.310\mu\text{m}$ , and relative refractive index  $\Delta = 0.00995$ . Note that the odd coefficients are zero. Figure 1 shows the refractive index profile of the optical fiber, though the radius of the core must be specified; however, there is no need to specify the cladding radius  $b$  for these calculations.

The following remarks are important as pertaining to the above equation: point  $y = 0$  is singular, regular, and the solutions of the characteristic equations are integers. There are two initial conditions to define the solutions of the differential equation; however, if we discard the solutions that blow up at infinity, only the value  $a_0$  at  $y = 0$  is needed to obtain the series. In order to normalize our solutions  $a_0$  is chosen in our calculations to be equal to 1, and Table I has been constructed according to this criterion. In summary, the boundary conditions are:  $\Psi(\infty) = 0$  and  $\Psi(0) = 1$  if  $l = 0$ , and  $\Psi(0) = 0$  if  $l$  is a positive integer, that is,  $l = 1, 2$ , etc.

The variable for the asymptotic expansion is conveniently taken to be  $e^{-y}$ . Therefore, this expansion becomes

$$\Psi_a(y) = \sum_{r=1}^{\infty} b_r e^{-ry}, \tag{12}$$

where  $b_0$  is taken to be zero in order that  $\Psi_a(\infty)$  may become zero. In this way there is only one coefficient  $b_1$  to be defined in the previous series, because all the other coefficients depend on the value of the slope of the solution  $\phi(\rho)$  at  $\rho = 1$ . Once this slope has been found, the mapping to  $b_1$  is performed through the transformation previously defined in Eq.(9). The way to find that slope is by numerically solving

the equation using the shooting method [27], with the boundary initial condition of  $a_0 = 1$  at  $\rho = 0$ , and compelling the function  $\phi(\rho)$  to converge to zero for  $\rho = 1$ .

The values of the coefficients  $b_j$  of the asymptotic expansion for  $l = 0, 1, 2$  and  $m = 0, 1, 2, 3$  are shown in Table II.

TABLE I. Power series coefficients for the azimuthal eigenvalues  $l = 0, 1, 2$  and mth-mode NUMBERS  $m = 0, 1, 2, 3$ .

l	m	$a_0$	$a_2$	$a_4$	$a_6$	$a_8$
0	0	1	-2.6686	3.38977	-2.91395	1.84991
0	1	1	-9.6589	24.933	-33.6674	30.3563
0	2	1	-20.8472	110.261	-270.314	396.57
0	3	1	-36.8984	341.983	-1428.46	3431.86
1	1	1	-7.24176	18.554	-26.274	25.0029
1	2	1	-14.0239	66.6294	-163.257	250.397
1	3	1	-23.2721	181.603	-716.865	1726.75
2	1	1	-6.68592	17.5678	-26.3609	26.7432
2	2	1	-12.0049	64.8492	-136.844	220.064
2	3	1	-18.9826	135.933	-524.219	1280.35

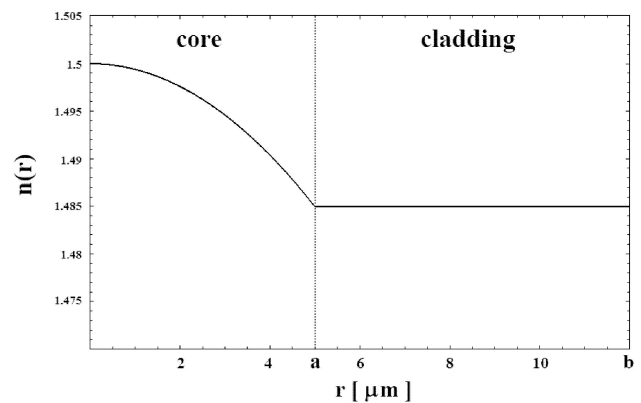


FIGURE 1. Refractive index profile of the optical fiber as a function of radius  $r$ ,  $a = 5\mu\text{m}$  is the radius of the core, and  $b$  is the cladding radius.

TABLE II. Asymptotic expansion coefficients for the azimuthal eigenvalues  $l = 0, 1, 2$  and mth-mode numbers  $m = 1, 2, 3$ .

l	m	$b_1$	$b_2$	$b_3$	$b_4$	$b_5$	$b_6$	$b_7$	$b_8$
0	0	0.6179	0.3089	1.7587	-1.7213	1.3071	-3.4137	3.3173	-2.75373
0	1	-1.5838	-0.7919	2.8732	8.1022	0.0419	-7.8231	-8.3976	4.2790
0	2	2.2049	1.1025	-20.4468	-19.5031	52.1783	77.7168	-46.1255	-132.135
0	3	-2.6530	-1.3265	52.9923	37.6616	-307.62	-286.198	808.457	971.288
1	1	-0.5002	-0.2501	2.4332	3.2386	-2.9311	-7.5344	-1.0254	7.6937
1	2	0.4587	0.2293	-6.3794	-5.0437	25.4249	28.1298	-43.9364	-69.2621
1	3	-0.4158	-0.2079	10.9099	7.1358	-84.0269	-68.1663	299.64	296.446
2	1	-0.2146	-0.1073	1.7342	1.6273	-3.9848	-5.7906	3.4866	9.4386
2	2	0.1453	0.0726	-2.7212	-1.8755	14.9004	13.2321	-37.6614	-42.772
2	3	-0.1052	-0.0526	3.4394	2.0925	-33.2183	-23.8442	150.567	126.088

TABLE III. Parameters  $p_i$ 's of the two-point quasi-rational approximants, for the azimuthal eigenvalues  $l = 0, 1, 2$  and mth-mode numbers  $m = 0, 1, 2, 3$ .

l	m	$p_0$	$p_1$	$p_2$	$p_3$	$p_4$	$p_5$	$p_6$	$p_7$	$p_8$
0	0	0.6179	0.1569	1.2289	-1.4048	0.315	0.0146	-	-	-
0	1	1.584	1.525	1.561	3.6737	-6.9425	2.4101	-	-	-
0	2	2.205	-4.528	-12.588	24.896	8.546	-28.804	10.906	-	-
0	3	-2.653	5.889	39.311	-86.899	-91.159	258.438	-29.654	-164.886	73.126
1	1	-0.500	0.973	0.996	-1.533	-1.474	2.132	-0.593	-	-
1	2	0.459	-1.194	-4.020	11.759	1.043	-22.727	19.817	-5.138	-
1	3	-0.416	1.584	6.521	-31.214	10.384	102.560	-174.559	109.681	-24.541
2	1	-0.215	0.413	1.047	-1.885	-0.849	1.908	0.397	-1.150	0.335
2	2	0.145	-0.478	-1.602	6.621	-1.914	-16.018	23.715	-13.033	2.563
2	3	-0.105	0.431	2.086	-10.667	3.689	42.819	-80.259	55.953	-13.946

TABLE IV. Parameters  $q_i$ 's of the two-point quasi-rational approximants, for the azimuthal eigenvalues  $l = 0, 1, 2$  and mth-mode numbers  $m = 0, 1, 2, 3$ .

l	m	$q_1$	$q_2$	$q_3$	$q_4$	$q_5$	$q_6$	$q_7$	$q_8$
0	0	-0.24594	-0.73429	1.57908	-0.99027	0.3201	-	-	-
0	1	-1.46303	1.55997	-0.63802	0.07458	0.11043	-	-	-
0	2	-2.55364	4.84114	-5.96457	5.49909	-3.1196	0.93054	-	-
0	3	-2.71981	6.51649	-10.6335	15.2787	-17.4547	16.676	-10.6535	3.50395
1	1	-2.44535	4.09631	-4.40347	3.38235	-1.58464	0.38568	-	-
1	2	-3.10195	6.69354	-9.85432	10.7551	-7.76077	3.30417	-0.55633	-
1	3	-4.30862	12.7086	-27.1731	46.038	-57.7928	49.1245	-24.5294	5.52864
2	1	-2.42578	4.41721	-5.44469	5.41243	-4.03907	2.30213	-0.85586	0.17594
2	2	-3.78673	9.59381	-17.2342	23.6842	-23.7457	16.3963	-6.86105	1.35102
2	3	-4.59566	15.1605	-36.5257	71.6558	-110.945	120.291	-75.6813	20.6874

### 3. Two-Point quasi-rational approximations for the solutions

The power series and asymptotic expansions previously found determine the form of the approximations to be used in this problem. The strategy of these quasi-rational approximants is to build an analytic bridge between the power series and the asymptotic expansion, to obtain a unique analytic expression using the coefficients of both expansions. The accuracy of the analytic approximations obtained with this procedure is high for the whole range of values, even in the region where both expansions are not convergent. The results are usually good for all values of the parameters, and are independent of the radius of convergence of each expansion.

One of the differences of the two-point quasi-rational approximant and the two-point Padé method is that a power series and an asymptotic expansion are used, instead of two power series. Consequently, instead of using only fractional functions, we are forced to introduce non-fractional functions, which we have called auxiliary functions, in order to

reproduce the singularities of the exact functions. The golden rule is that the function and the approximant should have the same singularities in the region of interest. Undesirable singularities that might appear in the approximant must be located outside of that region. Thus the auxiliary functions must be chosen in such a way that the undesirable singularities are located in the negative axis or in the left-hand complex plane. Another important advantage of the two-point quasi-rational approximants with respect to the Padé method is better accuracy for an equal number of parameters, and therefore the system of equations to obtain those parameters is simpler.

In this problem, the auxiliary function for the approximants will be  $e^{-y}$  and the variable of expansion  $e^{-y} = 1 - \rho$ . For an approximant of order  $s$ , that is, a polynomial of degree  $s$  in the numerator, the form of the approximant will be

$$\Psi_{approx}(y) = e^{-ly} \left( \frac{\sum_{i=0}^s p_i e^{-iy}}{1 + \sum_{h=1}^s q_h e^{-hy}} \right) \quad (13)$$

The  $(2s + 1)$  parameters  $p_i$ 's and  $q_h$ 's will be determined from the  $(2s + 1)$  coefficients coming from the power se-

ries and asymptotic expansions previously found. There are several possibilities; however, the best results are usually obtained when the number of coefficients from the power series is about the same as that of the asymptotic expansions. In Tables III and IV, the parameters of the approximants with the highest accuracy are shown. The  $p_i$ 's are in Table III and  $q_h$ 's are in Table IV. The procedure followed to obtaining these Tables is better explained by taking a particular case; for instance, let us explain how the  $p_i$ 's and  $q_h$ 's are obtained for the case  $l = 1$  and  $m = 2$ . The order of the approximant is seven and we have 15 unknowns, eight  $p_i$ 's and seven  $q_h$ 's ( $p_0$  to  $p_7$  and  $q_1$  to  $q_7$ ). Eight equations are obtained by equalizing the coefficients of the first eight terms of the power expansion in  $y$ , obtained as

$$\left[ 1 + \sum_{h=1}^7 q_h \left( \sum_{k=1}^7 \frac{(-1)^k h^k y^k}{k!} \right) \right] \left( y^l \sum_{i=0}^7 a_i y^i \right) = \left( \sum_{t=0}^7 \frac{(-1)^t t^l y^t}{t!} \right) \left( \sum_{i=0}^7 p_i \left( \sum_{k=0}^7 \frac{(-1)^k i^k y^k}{k!} \right) \right) + O(y^8), \quad (14)$$

where  $l = 1$ , but we have kept  $l$  as a letter in order to clarify the method. The sum over  $k$  and  $t$  correspond to the first eight coefficients of the power expansion of  $e^{-hy}$ ,  $e^{-iy}$  and  $e^{-ly}$ . These equations correspond to the information corresponding to small values of  $y$ .

In order to introduce the information coming for large values of  $y$ , that is, values of  $r$  near  $a$ , we need use the asymptotic expansion. Here we must to equalize the first seven coefficients of the exponentials as follows

$$\left( 1 + \sum_{h=1}^7 q_h e^{-hy} \right) \left( \sum_{j=1}^7 b_j e^{-jy} \right) = e^{-ly} \left( \sum_{i=1}^7 p_i e^{-iy} \right) + O(y^8). \quad (15)$$

In this way a linear system of 15 equations with 15 unknowns is obtained, and the results can be seen in the five rows of Tables III and IV.

As we noticed before, we have tried different arrangements, increasing the number of equations from the power series and decreasing those of the asymptotic expansions, and viceversa, but the best result is the one shown. Arrangements decreasing the number of exponentials in the numerator and increasing those in the denominator, and viceversa, have also been tested, but if the number of unknown parameters is fixed, better accuracy is obtained if there is an equal number of exponentials in the numerator and denominator as shown in Eq. (13).

Once the approximants are determined using the variable  $y$ , the approximant in  $\rho$  or  $r/a$  is obtained in a straightfor-

ward manner:

$$\begin{aligned} \phi_{approx}(\rho) &= (1 - \rho)^l \left( \frac{\sum_{i=0}^s p_i (1 - \rho)^i}{1 + \sum_{h=1}^s q_h (1 - \rho)^h} \right) \\ &= \left( 1 - \frac{r}{a} \right)^l \left( \frac{\sum_{i=0}^s p_i \left( 1 - \frac{r}{a} \right)^i}{1 + \sum_{h=1}^s q_h \left( 1 - \frac{r}{a} \right)^h} \right). \end{aligned} \quad (16)$$

### 4. Results

In this work, the approximants  $\phi_{approx}(\rho)$  for  $l = 0, 1, 2$  and  $m = 0, 1, 2, 3$  have been calculated. The order of each approximant increases until the accuracy of the approximation seems enough for most applications. Since the most important function  $\Psi(r)$  is for  $l = 0$ , these approximants are obtained with higher accuracy than those for  $l = 1$  and  $l = 2$ .

Figure 2, the function and the approximant for  $l = 0$ ,  $m = 0$  are shown. Both functions coincide on this scale. However the difference between both functions is given in Fig. 3, amplified with a  $10^4$  scale factor. The approximant in these figures has been obtained with a fifth-degree polynomial. The maximum absolute error is about  $0.44 \times 10^{-4}$ .

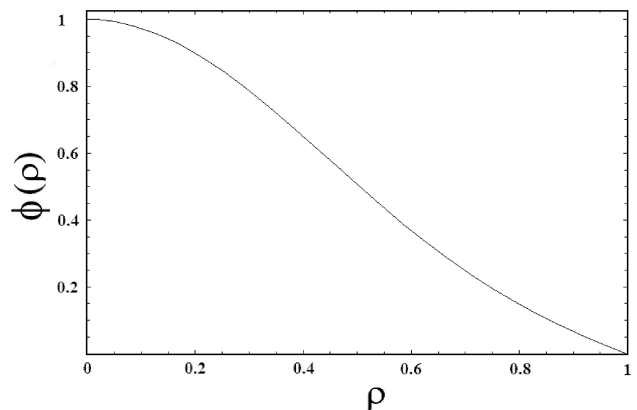


FIGURE 2. Two-point quasi-rational approximations of the radial wave solution  $\phi(\rho)$  as a function of the dimensionless radius  $\rho$  of the fundamental mode  $l = 0$  and  $m = 0$ .

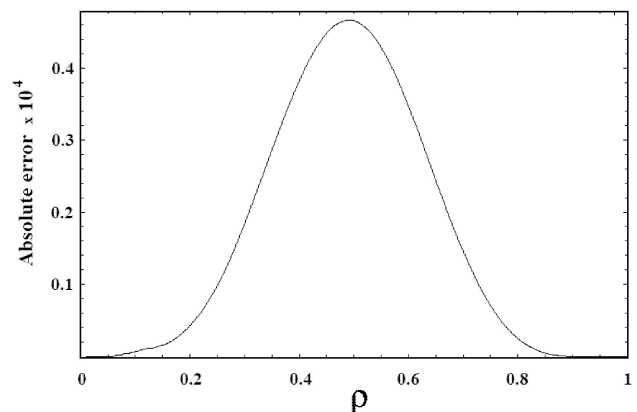


FIGURE 3. Amplified absolute error of the two-point quasi-rational approximants for the scalar wave function  $\phi(\rho)$  versus the dimensionless radius  $\rho$  of the fundamental mode  $l = 0$  and  $m = 0$ , after amplification by a factor of  $10^4$ .

Figure 4, the functions and approximants for  $l = 0$  and  $m = 1, 2$  and 3 are shown. On this scale, both functions, the exact one and the approximate one are coincident. A dashed line is used for the mode  $m = 1$ , a dotted line for  $m = 2$ , and a dot-dashed line for  $m = 3$ . For  $l = 0$ , the mode  $m = 1$  presents only a minimum,  $m = 2$  shows a minimum and a maximum, and  $m = 3$  has two relative minima and one maximum.

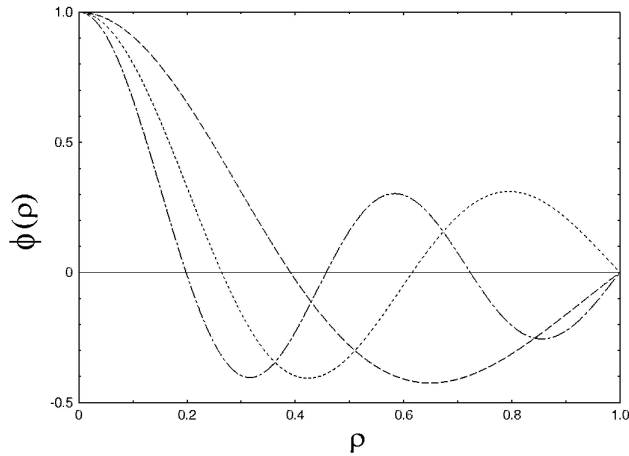


FIGURE 4. Amplified absolute errors of the two-point quasi-rational approximants for the scalar wave function  $\phi(\rho)$  versus the dimensionless radius  $\rho$ . The dashed curve (- -) corresponds to the error of the wave mode  $l = 0$  and  $m = 1$ , after amplification by a factor of  $10^4$ . Similarly the dotted curve ( $\cdot\cdot\cdot$ ) shows the error of the wave mode  $l = 0$  and  $m = 2$ , after amplification by a factor of  $10^3$ , and the dot-dashed curve ( $\cdot - - \cdot$ ) represents the error of the wave mode  $l = 0$  and  $m = 3$ , after amplification by a factor of  $10^2$ .

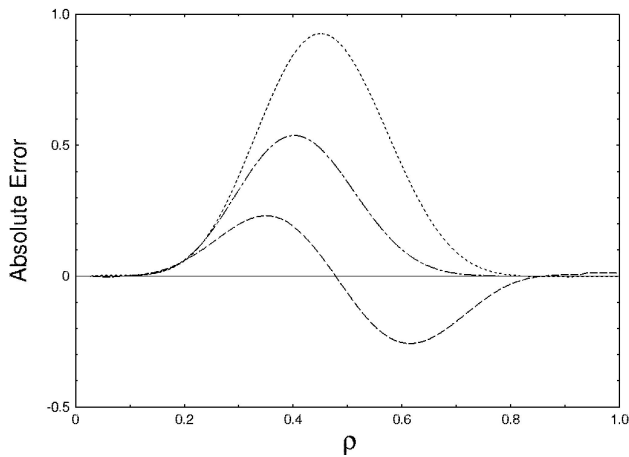


FIGURE 5. Amplified absolute errors of the two-point quasi-rational approximants for the scalar wave function  $\phi(\rho)$  versus the dimensionless radius  $\rho$ . The dashed curve (- -) corresponds to the error of the wave mode  $l = 0$  and  $m = 1$ , after amplification by a factor of  $10^4$ . Similarly the dotted curve ( $\cdot\cdot\cdot$ ) shows the error of the wave mode  $l = 0$  and  $m = 2$ , after amplification by a factor of  $10^3$ , and the dot-dashed curve ( $\cdot - - \cdot$ ) represents the error of the wave mode  $l = 0$  and  $m = 3$ , after amplification by a factor of  $10^2$ .

The absolute errors of the approximants in Fig. 4 are shown in Fig. 5. The same line-convention is kept here:  $m = 1$ , a dashed line;  $m = 2$ , a dotted line, and  $m = 3$ , a dot-dashed line. Since for the same values of  $\rho$  there are zeros for the function  $\phi(\rho)$ , in order to avoid infinite values, no relative errors can be shown and the figures show only absolute error. By overlapping Figs. 4 and 6, the relative errors can be illustrated, once the scale factors are taken into account. In Fig. 5, these scale factors are  $10^4$ ,  $10^3$  and  $10^2$  for  $m = 1, 2, 3$ , respectively. The maximum absolute errors

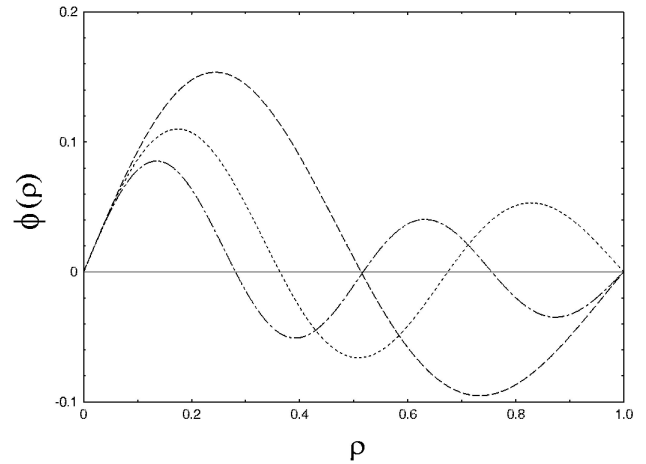


FIGURE 6. Two-point quasi-rational approximations of the radial wave solution  $\phi(\rho)$  as a function of the dimensionless radius  $\rho$ . Dashed (- -), dotted ( $\cdot\cdot\cdot$ ) and dot-dashed ( $\cdot - - \cdot$ ) curves correspond respectively to the three wave modes  $l = 1, m = 1$ ;  $l = 1, m = 2$  and  $l = 1, m = 3$ .

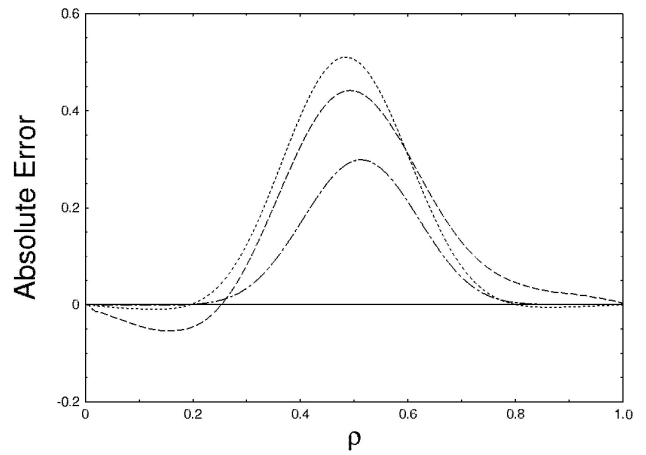


FIGURE 7. Amplified absolute errors of the two-point quasi-rational approximants for the scalar wave function  $\phi(\rho)$  versus the dimensionless radius  $\rho$ . The dashed curve (- -) corresponds to the error of the wave mode  $l = 1$  and  $m = 1$ , after amplification by a factor of  $10^4$ . Similarly, the dotted curve ( $\cdot\cdot\cdot$ ) shows the error of the wave mode  $l = 1$  and  $m = 2$ , after amplification by a factor of  $10^3$ , and the dot-dashed curve ( $\cdot - - \cdot$ ) represents the error of the wave mode  $l = 1$  and  $m = 3$ , after amplification by a factor of  $10^2$ .

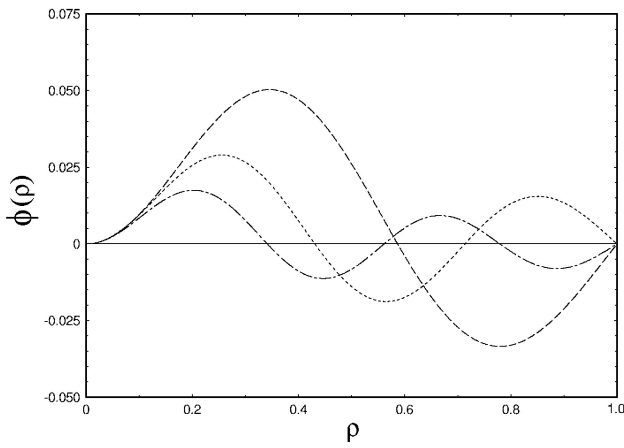


FIGURE 8. Two-point quasi-rational approximations of the radial wave solution  $\phi(\rho)$  as a function of the dimensionless radius  $\rho$ . Dashed (---), dotted (···) and dot-dashed (- · - ·) curves correspond respectively to the three wave modes  $l = 2, m = 1$ ;  $l = 2, m = 2$  and  $l = 2, m = 3$ .

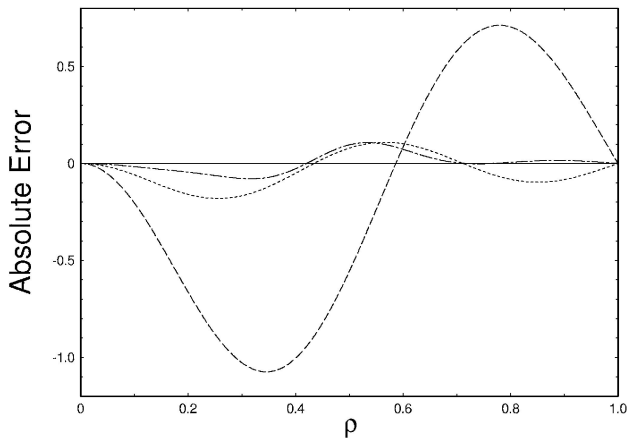


FIGURE 9. Amplified absolute errors of the two-point quasi-rational approximants for the scalar wave function  $\phi(\rho)$  versus the dimensionless radius  $\rho$ . The dashed curve (---) corresponds to the error of the wave mode  $l = 2$  and  $m = 1$ , after amplification by a factor of  $10^4$ . Similarly, the dotted curve (···) shows the error of the wave mode  $l = 2$  and  $m = 2$ , after amplification by a factor of  $10^3$ , and the dot-dashed curve (- · - ·) represents the error of the wave mode  $l = 2$  and  $m = 3$ , after amplification by a factor of  $10^2$ .

are  $0.23 \times 10^{-4}$ ,  $0.9 \times 10^{-3}$  and  $0.53 \times 10^{-2}$  for  $m = 1, 2, 3$ , respectively. Though the maximum errors tend to be in the central region, near the center the error of  $l = 0, m = 1$  is very near to zero.

The criteria used in Figs. 4 and 5 are followed in Figs. 6 and 7, for  $l = 1$  and the  $m = 1, 2, 3$  and latter in Fig. 8 and Fig. 9, for  $l = 2$  and  $m = 1, 2, 3$ . The scale factors in Fig. 7 are the same as that in Fig. 5; however, the largest errors are now:  $0.44 \times 10^{-4}$  for  $m = 1$ ,  $0.5 \times 10^{-3}$  for  $m = 2$  and  $0.29 \times 10^{-2}$  for  $m = 3$ . Here the largest errors are more centered than in the case for  $l = 0$ , described in Fig. 5. Referring now to  $l = 3$ , described in Figs. 8 and 9, the scale factors of the absolute errors are now different from previous ones,

and they are  $10^3$ ,  $10^2$ , and  $10^2$  for  $m = 1, 2, 3$ , respectively. The maximum errors are now  $1.1 \times 10^{-3}$ ,  $0.08 \times 10^{-2}$  and  $0.18 \times 10^{-2}$  for  $m = 1, 2, 3$ , respectively. Now, the maximum errors are not so centered as in the previous cases,  $l = 0, 1$ .

Another way to find approximants for the solutions of the differential equation considered here is by using two-point Padé methods, instead of the method previously described. In this method, the form of the approximants is similar to those in Eq. (16). However, the way to calculate the parameters is by two series expansions: one around  $\rho = 0$ , and the other around  $\rho = 1$ . We have determined the parameters  $p_i$  and  $q_h$  with this method for all the cases considered. Using the same number of parameters  $p_i$  and  $q_h$ , we have determined those parameters by the two methods, two-point quasi-rational and two-point Padé. After that, we proceeded to compare the accuracy of both approximants and we found that the accuracy of the one presented here is always better than those described in the Appendix. In general, that accuracy is about one or two orders of magnitude higher (the order of magnitude considered here is a factor of 10).

### 5. Conclusions

Analytic approximated solutions for wave propagation in quadratic graded-index optical fibers has been found. The accuracy of the approximants found here is much better than previous approximations found for other authors through WKB or any other method. No difference between approximated and computed functions can be found for figures with regular sizes. The absolute errors for  $m = 0, 1$  and  $l = 0, 1$  are always lower than  $10^{-4}$ , and close to  $10^{-3}$  for  $l = 2$ . For  $m = 2$ , the errors are always lower than  $10^{-3}$  for  $l = 0, 1, 2$ . For  $m = 3$ , the maximum error is  $10^{-2}$ , for  $l = 0, 1, 2$  and the errors are lower than  $10^{-2}$  for  $l = 0, 1$ . Clearly the accuracy of our approximant is very good and it can be used for most of the actual applications. The approximated solution can be derived and integrated like symbolic functions if needed.

Our approximants are obtained by using two-point quasi-rational methods, just described. The accuracy of the approximants using two-point Padé method is always lower than those obtained here for approximants of an equal number of parameters to be determined.

The main idea of those approximants is to combine rational functions with auxiliary functions in such a way that the singularities of the approximated function coincides with those of the actual function in the region of interest. Keeping this in mind, the method presented here can be applied to other multimode optical fibers with a graded index profile with different structures from the parabolic case considered here.

### Acknowledgments

We would like to thank the referee for several suggestions which improved our first manuscript.

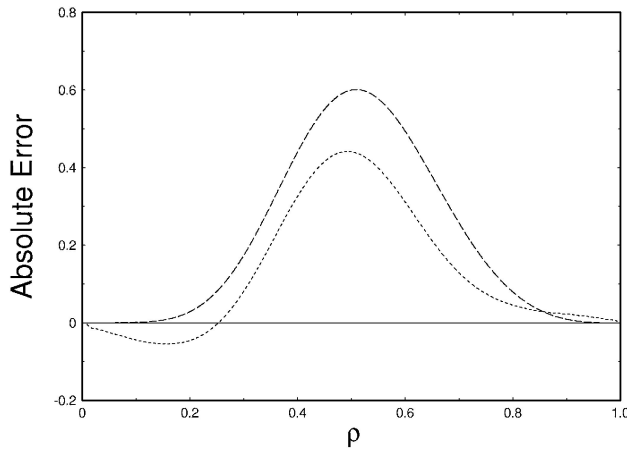


FIGURE 10. Amplified absolute errors of the two-point Padé method and the two-point quasi-rational approximants for the scalar wave function  $\phi(\rho)$ , versus the dimensionless radius  $\rho$ . The wave mode  $l = 1$  and  $m = 1$  is represented by a dashed curve (- -) in the case of two-point Padé approximation errors after amplification by a factor of  $10^2$ , and the dotted curve ( $\cdots$ ) corresponds to the error of the two-point quasi-rational approximation, after amplification by a factor of  $10^4$ .

**Appendix**

A different form for the approximated solution to Eq. (7) has been considered. The form of this approximated solution is a little simpler than that proposed in the main text; however, it is not so efficient. Here the word “efficient” is used in the sense of obtaining a given accuracy using the minimum number of unknown parameters in the approximant.

Here the form of the approximants will be

$$\tilde{\phi}(\rho) = (1 - \rho) \rho^l \frac{\sum_{i=0}^s \tilde{p}_i (1 - \rho)^i}{1 + \sum_{j=1}^s \tilde{q}_j (1 - \rho)^j}, \tag{17}$$

where  $\tilde{p}_i$  y  $\tilde{q}_j$  are parameters to be determined. The selection of the form is done considering that the function must be one at  $\rho = 0$  and zero at  $\rho = 1$ , for  $l = 0$ , and the function must be zero at  $\rho = 0$ , and  $\rho = 1$  for  $l = 1$  and 2. Furthermore, near zero the behavior of the function should be like  $\rho^l$ .

The auxiliary function  $(1 - \rho)$  is factored, because of the boundary condition that the function  $\Psi(r)$  must be zero at the surface of the cylinder  $r = a$ , that is,  $\phi(1) = 0$ . There is some freedom in the choice of the higher degree of the numerator and denominator. However, we have found that the best results are obtained when both degrees are equal or about the same.

Now, the power expansion around  $\rho = 0$  and  $\rho = 1$  must be found. The point  $\rho = 0$  is a singular regular point of the equation and  $\rho = 1$  is a regular point. We know that the straightforward calculation described before leads to

$$\tilde{\phi}(\rho)_0 = \tilde{a}_0 \rho^l \left( 1 + \sum_{k=1}^{\infty} \tilde{a}_k \rho^k \right). \tag{18}$$

Here, as usual there are two series which depend on the roots of the characteristic equation. However, here both solutions of the characteristic equation are equal integers. Therefore,

the well known procedure gives two solutions, one is logarithmic and the other is algebraic. We will not take into account the logarithmic solution because of the finite value of  $\phi(\rho)$  at the axis, that is, for  $\rho = 0$ .

Similarly at the boundary  $\rho = 1$ , the series expansion will be

$$\tilde{\phi}(\rho)_1 = \tilde{c}_0 (1 - \rho) \left[ 1 + \sum_{\gamma=1}^{\infty} \tilde{c}_\rho (1 - \rho)^\gamma \right]. \tag{19}$$

In order to find the parameters  $\tilde{p}_i$  and  $\tilde{q}_i$ , the previous series [Eqs. (18) and (19)] are multiplied by the denominator of the approximant

$$\left[ 1 + \sum_{j=1}^s \tilde{q}_j (1 - \rho)^j \right].$$

In the case of the power series of Eq. (19), before finding the product, the denominator is expanded in powers of  $\rho$ . The second step is to identify the coefficients of those expansions with the corresponding ones in the denominator expansion

$$\sum_{i=0}^s \tilde{p}_i (1 - \rho)^i.$$

In order to find unique values of  $\tilde{p}_i$  and  $\tilde{q}_i$ , the number of equations must be equal to the number of unknown parameters  $\tilde{p}_i$  and  $\tilde{q}_i$ . To be precise, the number of equations must be  $(2s + 1)$ ; that is, the number of coefficients to be equalized for the powers in  $\rho$  plus those for powers in  $(1 - \rho)$  must be  $(2s + 1)$ .

There is no need to write down the values of all the parameters  $\tilde{p}_i$  y  $\tilde{q}_j$  for the two-point Padé method, since the approximants to be used are those described above. However, to illustrate the results, the case  $l = 1$  and  $m = 1$  will be described in detail. In this case the approximant is of the sixth order, that is, there are sixth-degree polynomials of in the numerator and denominator, as the approximant described in the main text. For the two-point Padé method, the power series around  $\rho = 0$  and  $\rho = 1$ , for  $l = 1$  and  $m = 1$ , are

$$\begin{aligned} \tilde{\phi}(\rho)_0 = \rho - 7.2417\rho^3 + 18.554\rho^5 - 26.279\rho^7 \\ + 25.0029\rho^9 + \dots, \end{aligned} \tag{20}$$

$$\begin{aligned} \tilde{\phi}(\rho)_1 = -0.5002(1 - \rho) - 0.2501(1 - \rho)^2 \\ + 2.5164(1 - \rho)^3 + 3.3634(1 - \rho)^4 \\ - 3.0491(1 - \rho)^5 - 7.9842(1 - \rho)^6 + \dots \end{aligned} \tag{21}$$

Figure 10 illustrates the errors, and they are compared with the errors found in the main text. In order to get a clear picture of both errors, the scale factor of both errors are different, and the one shown in the main text has an extra factor of 100 compared with that of the two-point Padé method, that is, the scale factors are  $10^4$  and  $10^2$ . The maximum errors are  $0.6 \times 10^{-2}$  and  $0.44 \times 10^{-4}$ , for the two-point Padé method and for the two-point quasi-rational approximant, respectively.

1. P.K. Cheo, *Fiber Optics and Optoelectronics* (Prentice Hall Series In Solid Physical Electronics, Second Edition, 1990) Ch. 4.
2. M. Young, *Optics and Lasers: Including Fibers and Optical Waveguides* (Springer-Verlag, Berlin Heidelberg, Fourth Revised Edition, 1993) Ch. 10.
3. C.C. Davis, *Lasers and Electro-Optics, Fundamentals and Engineering* (Cambridge University Press, 1996) Ch. 17.
4. W. Streifer and C.N. Kurtz, *J. Opt. Soc. Am.* **57** (1967) 779.
5. S. Kawakami and Jun-Ichi Nishizawa, *IEEE Trans. Microwave Theory Tech.* **MIT-16** (1968) 814.
6. E.G. Jhonson, J. Stack and C. Koehler, *J. Lightwave technol.* **19** (2001) 753.
7. F.C. Mc Neillie, J. Thomson, and I.S. Ruddock, *Eur. J. Phys.* **25** (2004) 479.
8. J.W. Rose and S.S. Mitra, *Optics Letter* **6** (1981) 446.
9. A.H. Hartog and M.J. Adams, *Opt. Quant. Elec.* **9** (1977) 223.
10. G.A. Jr. Baker and P.R. Graves-Morris, *Padé Approximants, Part I: Basic Theory* (Encyclopedia of Mathematics and its Applications Vol 14) (Cambridge: Cambridge University Press, 1981).
11. P. Martín, G. Donoso and J. Zamudio, *J. Math. Phys.* **21** (1980) 280.
12. E. Chalbaud and P. Martín, *J. Math. Phys.* **25** (1984) 1268.
13. E. Chalbaud and P. Martín, *J. Math. Phys.* **27** (1986) 699.
14. P. Martín and L. A. Guerrero, *J. Math. Phys.* **26** (1985) 705.
15. K. Visentin and P. Martín, *J. Math. Phys.* **28** (1987) 330.
16. A.L. Guerrero and P. Martín, *J. Comput. Phys.* **77** (1988) 276.
17. P. Martín and A.L. Guerrero, *J. Comput. Phys.* **85** (1989) 487.
18. P. Martín, and G. Baker, *J. Math. Phys.* **32** (1991) 1470.
19. E. Chalbaud and P. Martín, *J. Math. Phys.* **33** (1992) 2483.
20. P. Martín, R. Pérez, and L.A. Guerrero, *J. Comput. Phys.* **99** (1992) 337.
21. L. Brualla and P. Martín, *J. Phys. A: Math. Gen.* **34** (2001) 9153.
22. P. Martín and J. Puerta, *Eur. J. Phys.* **12** (1991) 1992.
23. P. Martín, J.J. Rodríguez-Núñez, and J.L. Marquez, *Phys. Rev. B* **45** (1992) 8359.
24. E. Castro and P. Martín, *J. Phys. A: Math. Gen.* **33** (2000) 5321.
25. C.L. Ladera and P. Martín, *J. Comput. Phys.* **73** (1987) 481.
26. L.C. Ladera and P. Martín, *J. Phys. A: Math. Gen.* **34** (2001) 4571.
27. S. Nakamura, *Applied Numerical Method with Software* (Englewood Cliffs, N J: Prentice Hall, 1992) Ch. 9.